Cataglyphis desert ants improve their mobility by raising the gaster

Robert M. McMeeking [a,b,c,d], Eduard Arzt [a,*], Rüdiger Wehner [e,f]

[a] INM—Leibniz Institute for New Materials and Saarland University, Campus D2 2, D-66123 Saarbrücken, Germany
[b] Department of Mechanical Engineering, University of California, Santa Barbara, CA 93106, USA
[c] Materials Department, University of California, Santa Barbara, CA 93106, USA
[d] School of Engineering, Aberdeen University, King's College, Aberdeen AB24 3UE, Scotland
[e] Brain Research Institute, University of Zürich, Winterthurerstrasse 190, CH-8057 Zürich, Switzerland
[f] Biocenter, University of Würzburg, Am Hubland, D-97074 Würzburg, Germany

ARTICLE INFO

ABSTRACT

We analyze theoretically the moment of inertia of the desert ant Cataglyphis (C. bicolor and C. fortis) around a vertical axis through its own center of mass when the animal raises its gaster to a vertical position. Compared to the value when the gaster is horizontal, the moment of inertia is reduced to one half; this implies that when increasing its angular acceleration the ant need apply only half the level of torque when the gaster is raised, compared to when the gaster is lowered. As an example, we analyze the cases of an ant running on circular and sinusoidal paths. In both cases, the ant must apply a sideways thrust, anti-roll and anti-pitch torques to avoid toppling, and, on the circular path when accelerating and throughout the sinusoidal trajectory, a torque to enable turning as the path curves. When the ant is accelerating in a very tight circle or running on a very narrow sinusoidal path, in which the amplitude of the sinusoid is less than the length of the ant's body, the forces required for the turning torque can equal and exceed those required for the sideways thrust, and can be reduced significantly by the ant raising the gaster, whereas the foot-thrust for the anti-roll and anti-pitch torques rises only modestly when the gaster is up. This suggests that there may be an evolutionary advantage for employing the gaster-raising mode of locomotion, since this habit will allow desert ants to use lower forces and less energy, and perhaps run faster on more tortuous paths.

© 2011 Elsevier Ltd. All rights reserved.

1. Introduction

Some Saharan desert ants of the genus Cataglyphis, especially those belonging to the bicolor species group (e.g., C. bicolor) and the albicans species group (e.g., C. fortis) are able to raise the gaster until its major axis is vertical (Fig. 1). This position contrasts with the lowered orientation in which the major axis of the gaster is nearly horizontal, and aligned with the ant's other body parts (Wehner, 1982, 1983). The ability of raising the gaster is associated with a nodiform or cubiform rather than squamiform petiolus (Fig. 2) (Wehner et al., 1994). The squamiform petiolus, which is typical for formicine ants in general, is still present in some more original Cataglyphis species such as C. emmae, the members of the cursor species group, and C. bombycina (Agosti, 1990). These species – most remarkably C. bombycina, the "silver ant" of the Sahara, the Sinai and the deserts of the Arabian Peninsula – are unable to raise the gaster. Even though they reach high running speeds, they proceed along almost straight lines and decelerate or even stop when turning (Wehner and Wehner, 1990). In contrast, C. bicolor and C. fortis are able to both

elevate the gaster and perform remarkably tortuous runs, during which they reach high rates of turning with the gaster elevated.

Here we test the hypothesis, promoted almost 30 years ago (Wehner, 1982, 1983), that the erect position of the gaster reduces the ant's moment of inertia and hence facilitates maneuverability. A lowered moment of inertia would allow the ant to perform fast turns with reduced levels of torque generated from the motion of its legs. We investigate this concept quantitatively by modeling the moment of inertia for the ant with its gaster raised and lowered. In addition, we consider an ant running on circular and sinusoidal paths to estimate the relative levels of torque and foot-thrust required when the gaster is erect and lowered.

1.1. Geometric model of Cataglyphis

As illustrated in Fig. 2, Cataglyphis has four main body parts. They are the head, the thorax (alitrunk), the petiole (petiolus) and the gaster (metamosa) (Wehner, 1983; Wehner et al., 1994). In addition, there are legs, mandibles, antennae and other small appendages, whose geometry we ignore for the purpose of estimating the insect's moment of inertia. The dimensions (defined in Fig. 2) and mass of each body part are listed in

Fig. 1. Sketches of *Cataglyphis fortis* with its gaster in a near vertical position as adopted when running through tight turns. From Wehner (1982).
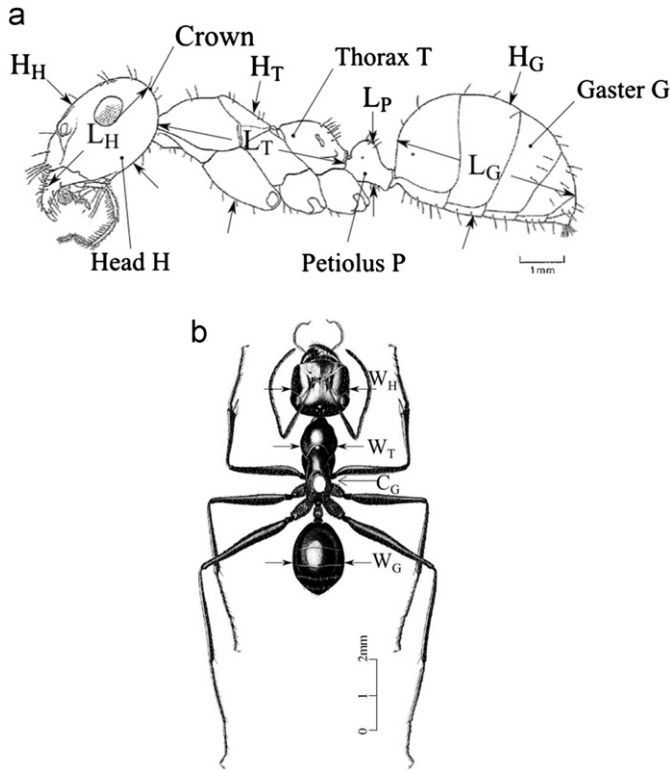

Fig. 2. (a) Lateral and (b) dorsal view of *Cataglyphis bicolor* and *Cataglyphis fortis*, respectively. The body parts (head H, thorax T, petiolus P, gaster G) and measured dimensions (see Table 1) are indicated. The white dot in (b) marks the center of gravity when the gaster is in a horizontal position. Drawings adapted from Wehner (1983) and Wehner et al. (1994).

Table 1 for workers of *C. bicolor* and *C. fortis*. The mass of each body part was measured on freshly killed animals, and all appendages of the head were attached. Negligible desiccation occurred in the few seconds involved in handling, as is confirmed by the data for wet brains provided by Wehner et al. (2007). In each case, measurements were made on 3 animals, and the mean values used to prepare Table 1. The measured ants were all taken while on foraging runs outbound from the nest, and therefore following tortuous paths. As a consequence, the dimensions and masses in Table 1 are those relevant to the ant's inertia when it is making its rapid turns. After securing food, the ant returns to the nest on relatively straight paths. The inertia of the animal carrying a food item is not relevant to our study.

In view of the shapes of the body parts, we model the head, thorax and gaster as ellipsoids and the petiolus as a sphere. The lay-out of our geometric model is shown in various states in Fig. 3. As can be seen in Fig. 2a, the head is oriented so that its short axis, (*i.e.* height) is oriented at approximately 45° to the horizontal axis of the ant (Wehner, 1982), which we define to be the *x*-axis (see Fig. 3a). The *y*-axis is parallel to the width dimension of all body

parts and the *z*-direction is vertical. The long axis (*i.e.* the length L_T) of the thorax is, in the first instance, assumed to be aligned with the *x*-axis, as illustrated in Fig. 3. We also consider the case where the thorax is inclined by $\phi = 20°$, sloping downwards from the head to the petioles. When the gaster is lowered, its long axis (*i.e.* the length L_G) is assumed to be aligned with the *x*-axis, as shown in Fig. 3a. When fully elevated, it is assumed to be vertically above the petiole, as shown in Fig. 3b. The gaster may be at an orientation intermediate to the horizontal and the vertical, in which case it will have an angle of inclination, ψ, to the horizontal as shown in Fig. 3c. Thus $\psi = 0$ is a horizontal gaster, whereas $\psi = \pi/2$ is a vertical one. The head is assumed to be attached to the thorax such that the center of its crown, as marked in Fig. 2, is vertically above the proximal end of the thorax. The origin of the Cartesian coordinate system is taken to lie at the center of mass of the ant in the *x–y* plane, as shown in Fig. 3a. Note that throughout this paper we use the general term "thorax" rather than "alitrunk" for the middle part (mesosoma) of the body. In the nomenclature of hymenopteran morphology "alitrunk" would be the more appropriate term (see also legend of Table 1).

1.2. Center of mass of the ant

We first compute the center of mass of the whole ant. We assume that the ant is running on level ground that is parallel to the horizontal *x–y* plane, uses all six feet, and is able to avoid toppling. The density of each body part is taken to be uniform within that body part, though the density of each is allowed to be unique. By symmetry, the center of mass will bisect the dorsal projection. In view of the assumptions of shape and uniformity of density, each body part has a center of mass central to it, so all such centers of mass also lie in the *x–z* plane. Furthermore, we assume that the centers of mass of each body part lie on the *x*-axis when the ant has its gaster held horizontal.

The distance from the mandibles to the center of gravity of the ant is L_C, as shown in Fig. 3, and is computed, by balancing gravitational moments (Goldstein, 1950) around the *y*-axis, according to

$$m_A L_C = m_H \frac{L_H}{2\sqrt{2}} + m_T \left(\frac{L_H}{\sqrt{2}} + \frac{L_T}{2} \cos\phi \right) + m_P \left(\frac{L_H}{\sqrt{2}} + L_T \cos\phi + \frac{L_P}{2} \right)$$
$$+ m_G \left[\frac{L_H}{\sqrt{2}} + L_T \cos\phi + \frac{L_P}{2} + \left(\frac{L_P}{2} + \frac{L_G}{2} \right) \cos\psi \right] \quad (1)$$

where m_A is the mass of the ant, and m_I is the mass of a body part, with subscript H representing the head, T the thorax, P the petiolus and G the gaster. Thus

$$m_A = m_H + m_T + m_P + m_G \quad (2)$$

The angle ϕ, as noted above, is the angle between the *x*-axis and the long axis of the thorax. It is taken to be zero for the purposes of the diagrams in Fig. 3.

The average *Cataglyphis bicolor* (*Cataglyphis fortis*) as characterized by the data in Table 1 has mass $m_A = 28.72$ mg (8.37 mg). The dimensions L_H, L_T, L_P and L_G are the major axes of the head, thorax, petiole and gaster, respectively. Their measures are depicted in Figs. 2 and 3. With the gaster and thorax horizontal, the ant's center of mass lies in the thorax near the thorax–petiole joint, at a distance of 0.222 mm (0.514 mm) from that junction. This distance represents 5% (20%) of the length of the thorax. This estimate agrees fairly well with an experimental measurement performed on *Cataglyphis bicolor*, in which the center of mass was found to be near the same junction, but displaced by about 10% of the thorax length (Zollikofer, 1988). When the gaster is vertical, the center of mass of the average *C. bicolor* (*C. fortis*) is quite near the center of the thorax, being 0.706 mm (0.112 mm) to the right of it in the views of Fig. 3. This distance is 16% (4% for *C. fortis*) of

Table 1
Dimensions and weights of body parts for (a) *Cataglyphis bicolor* and (b) *Cataglyphis bicolor*. The table presents the means of data obtained from 3 ants in each case. The more technical terms for thorax, gaster and petiole are alitrunk, metasoma and petiolus, respectively. For the definition of the dimensions, refer to Fig. 3.

| Body part	Length L mm	Width W mm	Height H mm	Mass m mg	Mass m % of ant's mass
(a) *Cataglyphis bicolor*					
Head	2.564	2.305	1.663	6.720	23
Thorax	4.431	1.816	1.678	6.307	22
Gaster	3.934	2.781	2.625	15.543	54
Petiole is approximately equiaxed with diameter 0.825 mm and mass 0.15 mg (0.5%).					
(b) *Cataglyphis fortis*					
Head	1.805	1.765	1.194	2.717	32
Thorax	2.655	1.232	0.986	1.677	20
Gaster	2.484	1.716	1.648	3.923	47
Petiole is approximately equiaxed with diameter 0.506 mm and mass 0.05 mg (0.6%).					
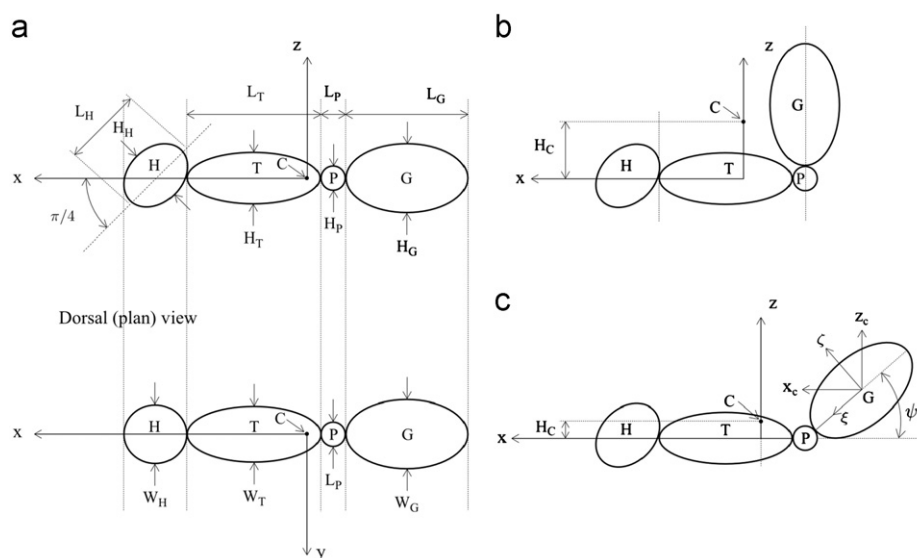
Fig. 3. Diagrams of 3 ellipsoids and a sphere used to model the body parts of the ant, and the coordinate system utilized. (a) Sagittal (elevation) and dorsal (plan) view, gaster horizontal. The head is inclined at 45° and the crown of the head is aligned above the proximal end of the thorax. (b) Sagittal (elevation) view of the ant model with its gaster vertical. (c) Sagittal (elevation) view of the ant model with its gaster at inclination angle ψ.

the length of the thorax. The x-coordinate positions of the centers of mass of *C. bicolor* and *C. fortis* for a few positions of the gaster when the thorax is horizontal are given in Table 2.

The raising of the gaster causes the ant's center of mass to rise above the x-axis. By balancing moments that would arise if gravity acted parallel to the x-axis, we deduce that the height, H_C, of the center of mass above the x-axis, when the thorax is horizontal and the gaster is vertical, is given by $H_C = 0.5(L_P+L_G)m_G/m_A$. For *C. bicolor*, $H_C = 1.288$ mm and when *C. fortis* is considered, $H_C = 0.701$ mm. Such elevation of the ant's center of mass upon gaster raising was identified by Dlusskij (1981) through use of a model constructed from paper. In general, with the thorax horizontal and the gaster at an angle ψ, the distance from the x-axis to the position of the center of mass on the z-axis is given by

$$H_C = \frac{m_G(L_P+L_G)\sin\psi}{m_A} \tag{3}$$

Results for this parameter are given also in Table 2, and its definition is clarified in Fig. 3c.

Table 2
Position of the center of gravity of (a) *Cataglyphis bicolor* and (b) *Cataglyphis fortis* with the thorax horizontal and the gaster at various angles.

Gaster angle ψ	Distance from the mandibles to the ant center of gravity L_C (mm)	Height of the center of gravity above its position with the gaster horizontal H_C (mm)
(a) *Cataglyphis bicolor*		
0	6.022	0
$\pi/8$	5.924	0.493
$\pi/4$	5.645	0.911
$3\pi/8$	5.227	1.190
$\pi/2$	4.734	1.288
$5\pi/8$	4.241	1.190
(b) *Cataglyphis fortis*		
0	3.417	0
$\pi/8$	3.364	0.268
$\pi/4$	3.212	0.496
$3\pi/8$	2.984	0.648
$\pi/2$	2.716	0.701
$5\pi/8$	2.448	0.648

1.3. Moment of inertia of the ant about its center of mass

When the ant is turning, it will have to apply a torque around its center of mass proportional to its angular acceleration times its moment of inertia relative to its center of mass (Goldstein, 1950). For clarity we summarize the formulation here to see how it is to be applied to each body part of the ant. Consider an ant spinning rigidly around the z-axis passing through its center of mass. The resulting acceleration of any point in the ant is

$$\frac{d\underline{v}}{dt} = \dot{\omega}(x\underline{j} - y\underline{i}) - \omega^2(x\underline{i} + y\underline{j}) \tag{4}$$

where $\underline{v}$ is the velocity vector, t is time, ω is the rate of rotation, or angular velocity, of the ant in radians per unit time, and $\dot{\omega}$ is the time rate of change of ω and is thus the ant's angular acceleration. The terms $\underline{i}$ and $\underline{j}$ are the unit base vectors for the Cartesian coordinate system in the x- and y-directions, respectively. The moment vector, $\underline{M}$, or torque, that must be applied by the ant to cause this acceleration is then given by

$$\underline{M} = \int_V \rho(x\underline{i} + y\underline{j}) \times \frac{d\underline{v}}{dt} dV = \dot{\omega}\underline{k} \int_V \rho(x^2 + y^2)dV = J\dot{\omega}\underline{k} \tag{5}$$

where V is the volume of the ant's body, ρ is the local density of the interior of the ant's body parts, $\times$ denotes the vector or cross product, and $\underline{k}$ is the unit base vector in the z-direction. The integral in the penultimate form in Eq. (5) is the moment of inertia, J, of the ant about its center of mass.

For any body part with volume V_I, ($I = H, T, P, G$ for head, thorax, petiolus and gaster, respectively), the contribution to the integral can be written as

$$\int_{V_I} \rho(x^2 + y^2)dV = \rho_I \int_{V_I} [(r_I + x_C)^2 + y_C^2]dV = m_I r_I^2 + \rho_I \int_{V_I} (x_C^2 + y_C^2)dV \tag{6}$$

where ρ_I is the density of the relevant body part, r_I is the distance along the x-axis from the center of mass of the ant to the position of the centroid of the body part in question, and (x_C, y_C, z_C) are Cartesian coordinates of points in the body part relative to an origin at the centroid of that body part. Thus the definition of r_I is such that $x = x_C + r_I$, while $y_C = y$. The parameter r_I is known as the radius of gyration of the body part (Goldstein, 1950). The linear terms in Eq. (6) are zero by definition of the centroid of the body part. The integral in the final form in Eq. (6) is the moment of inertia of the body part about its own center of mass. The final form is the well-known Steiner or parallel axis theorem (Goldstein, 1950).

For all body parts, the integral containing y_C in the final form in Eq. (6) is completed by the procedure

$$\rho_I \int_{V_I} y_C^2 dV = 2\rho_I \int_0^{y_o} y_C^2 A(y_C)dy_C = 2\pi\rho_I x_o z_o \int_0^{y_o} y_C^2 \left[1 - \left(\frac{y_C}{y_o}\right)^2\right]dy_C$$

$$= \frac{1}{20}m_I W_I^2 \tag{7}$$

where we take the ellipsoid in question to have semi-axes x_o, y_o, z_o. A is the area of the elliptical cross section in the sagittal plane at y_C and therefore having semi-axes $x_o\sqrt{1 - y_C^2/y_o^2}$ and $z_o\sqrt{1 - y_C^2/y_o^2}$. Given that the area of an ellipse is π times the product of the 2 semi-axes, and that the volume of an ellipsoid is $4\pi/3$ times the product of the 3 semi-axes, we obtain the result in Eq. (7). In addition we use $y_o = W_I/2$, where W_I is the width of the body part, as defined in Fig. 2 and tabulated in Table 1.

To allow for a gaster and a thorax that may be raised above the horizontal orientation, and to account for the head, we introduce a change of variables for x_C given by

$$x_C = \xi\cos\psi - \zeta\sin\psi \tag{8}$$

where the coordinates (ξ, ζ) are indicated in Fig. 3c. When x_C in Eq. (8) is squared, the term containing the product $\xi\zeta$ gives no contribution to the resulting integral, and we then deduce that

$$\rho_I \int_{V_I} x_C^2 dV = \frac{1}{20}m_I(L_I^2\cos^2\psi + H_I^2\sin^2\psi) \tag{9}$$

on similar grounds to those that gave us the result in Eq. (7). The expressions in Eqs. (7) and (9) give us outcomes that can be used for all body parts. For the head, we set $\psi = \pi/4$, for the thorax we use $\psi = \phi$, and for the petiolus we set $\psi = 0$. In the case of the gaster, ψ is its angle of inclination, allowing us to specify whether it is raised to fully vertical and beyond, lowered to horizontal, or in an intermediate positions.

Now we can formulate the moment of inertia for the ant as a whole. From the parallel axis theorem and the various results above, we obtain

$$J = m_H r_H^2 + \frac{1}{40}m_H(L_H^2 + H_H^2 + 2W_H^2) + m_T r_T^2$$

$$+ \frac{1}{20}m_T(L_T^2\cos^2\phi + H_T^2\sin^2\phi + W_T^2)$$

$$+ m_P r_P^2 + \frac{1}{10}m_P L_P^2 + m_G r_G^2 + \frac{1}{20}m_G(L_G^2\cos^2\psi + H_G^2\sin^2\psi + W_G^2) \tag{10}$$

With its thorax and gaster horizontal, i.e. $\phi = 0$ and $\psi = 0$, respectively, Cataglyphis bicolor has $r_H = 5.115$ mm; $r_T = 1.993$ mm; $r_P = 0.635$ mm; $r_G = 3.014$ mm, whereas Cataglyphis fortis has $r_H = 2.779$ mm; $r_T = 0.813$ mm; $r_P = 0.767$ mm; $r_G = 2.262$ mm. The results for the moment of inertia are then $J = 3.708 \times 10^{-3}$ g cm^2 for C. bicolor and $J = 0.455 \times 10^{-3}$ g cm^2 for C. fortis. We note that the head contributes 48% of the total moment of inertia in both animals, and the gaster around 45%. Thus the head and the gaster dominate the moment of inertia by having radii of gyration larger than the other body parts. The terms dependent on the radii of gyration for the head and the gaster account for, respectively, 47% and 38% of the total moment of inertia in the case of C. bicolor, and 46% and 44% in the case of C. fortis. If we divide J by the total mass of the ant, we obtain the square of the radius of gyration of the ant as a whole when its thorax and gaster are horizontal. This radius of gyration is equal to 3.59 mm in the case of C. bicolor and 2.33 mm in the case of C. fortis.

With the thorax horizontal and the gaster vertical, i.e. $\phi = 0$ and, $\psi = \pi/2$, respectively, C. bicolor has $r_H = 3.827$ mm; $r_T = 0.705$ mm; $r_P = r_G = 1.923$ mm, and C. fortis has $r_H = 2.078$ mm; $r_T = 0.112$ mm; $r_P = r_G = 1.468$ mm. The results for the moment of inertia are then $J = 1.815 \times 10^{-3}$ g cm^2 for C. bicolor and $J = 0.229 \times 10^{-3}$ g cm^2 in the case of C. fortis. As for the gaster horizontal situation, the head and gaster dominate the moment of inertia, with the head contributing about 55%, and the gaster around 40%, fractions that are little changed from those prevailing when the gaster is horizontal. The terms dependent on the radii of gyration for the head and the gaster account for, respectively, 54% and 32% in the case of C. bicolor and 51% and 37% when C. fortis is considered. Again, these fractions are little changed from those relevant to the gaster horizontal configuration. With the thorax horizontal and the gaster vertical, the radius of gyration of the ant as a whole is 2.51 mm for C. bicolor and 1.65 mm for C. fortis.

It is notable that the ant is able to reduce its moment of inertia around its center of mass by a significant amount by raising its gaster to a vertical position. For the average Cataglyphis bicolor, with data summarized in Table 1a, the moment of inertia with the gaster vertical is only 49% of the value prevailing when the gaster is horizontal. Similarly, for the average Cataglyphis fortis, with data summarized in Table 1b, the moment of inertia with the gaster vertical is only 50% of the value prevailing when the gaster

is horizontal. This means that during rapid running the ant can reduce the required torque from its legs, at a given angular acceleration, to a half of what would be required with the gaster horizontal.

To provide additional information, we have summarized in Table 3a the moment of inertia of *C. bicolor* with its thorax horizontal ($\phi=0$) and its gaster at various angles of inclination, and for *C. fortis* in Table 3b. Results are given as the value of the moment of inertia, and as a percentage of the moment of inertia that the ant possesses when its gaster is horizontal. Since the terms containing the radius of gyration of each body part dominate the expression in Eq. (10), we have, in addition, computed the result for the moment of inertia neglecting everything except those terms. This result is that obtained when each body part is treated as a point mass located at its center of gravity, and is so described in Table 3. It can be seen that the point mass result involves significant error, ranging from 8% to 17% in the case of *C. bicolor* and from 23% to 64% in the case of *C. fortis*. However, when expressed as a percentage of the result that pertains to the ant holding its gaster horizontal, the point mass result is remarkably good. However, the point mass result exaggerates the benefit of raising the gaster in terms of how much the moment of inertia is reduced. This feature arises because the moment of inertia of each body part around its own centroid becomes more important in the final result when the shape of the ant is compact. This outcome arises because in a compact shape the radii of gyration are relatively small.

No doubt there will be significant variation of ant morphology from the average values summarized in Table 1. However, it seems safe to assume that *Cataglyphis bicolor* and *Cataglyphis fortis* can generally half their moment of inertia about the center of mass when the gaster is raised from the horizontal to the vertical orientation. In addition, the ant can reduce its moment of inertia even further by drawing its gaster beyond the vertical so that it makes an acute angle with the axis of its thorax, *i.e.* the case of $\psi=5\pi/8$ that has been included in Table 3. At this angle of inclination of the gaster, the ant's moment of inertia around its center of mass is around 35% of the value that pertains to the gaster horizontal. *C. fortis* has been observed to bring its gaster to approximately such a position when running in a tortuous path. It is notable from Table 3 that, despite their different sizes, the percentage reduction in the moment of inertia for a given gaster angle of inclination is almost the same for both *Cataglyphis* species, indicating self-similar scaling of their biomechanics.

The ant usually holds its thorax at an angle of inclination such that its end proximal to the head is above the distal one, *i.e. $\phi \neq 0$*. To determine whether this has a significant effect on the results, we have repeated our calculations for the case of $\phi=\pi/9$, typical of an ant running on a straight path (Duelli, 1975). The results are presented in Table 4. In view of the fact that the point mass result exaggerates the advantage of lifting the gaster, we have omitted these results. The more compact shape that results when $\phi=\pi/9$ reduces the ant's moment of inertia slightly compared to that arising when the thorax is horizontal. When expressed as a percentage of the result for a horizontal gaster, there is almost no difference between the values in Table 4 for the inclined thorax and those in Table 3 for the case of a horizontal thorax. However, the advantage of raising the gaster is slightly improved when the thorax is inclined, a result that arises because the inclined thorax allows a more compact shape when the gaster is raised.

1.4. Estimate of forces and torques for a running ant

Assume that the ant runs forward on a flat, horizontal surface, defined as the x_1-x_2 plane. At any given instant, the position vector, $\underline{r}$, for its center of gravity in this plane is

$$\underline{r} = x_1\underline{e}_1 + x_2\underline{e}_2 + H\underline{k} \qquad (11)$$

where $\underline{e}_i$, $i=1,2$, are unit vectors parallel to the coordinate axes x_1 and x_2, H is the height of the ant's $x-y$ plane above the ground (*i.e.* the height of its legs), and $\underline{k}$ is the unit base vector parallel to the z-axis previously defined in conjunction with Eq. (5). Suppose that the ant controls the motion of a point P within it at position $(x,y,z)=(x_P,0,0)$ and thus not at its center of gravity. We assume that the point P is unaltered within the ant when the gaster is raised or lowered. We judge this to be appropriate since it seems likely that the ant controls the motion of a point somewhere in its thorax centered among its legs. It seems reasonable that when the gaster is raised or lowered, this point remains fixed in place in the thorax, perhaps in the middle of the line drawn between the hips of its 2 center legs. As a result, x_P will have different values when the gaster is raised and lowered, as the x, y, z coordinate system is such that the center of mass is always at $(0,0,H_C)$.

Table 3
Moment of inertia of (a) *Cataglyphis bicolor* and (b) *Cataglyphis fortis* with the thorax horizontal and the gaster at various angles. Results are given for the complete result from Eq. (9) and for the result when each body part is treated as a point mass located at its center of gravity.

Gaster angle ψ	Moment of inertia Eq. (9) J (g cm^2)	Moment of inertia % of J when gaster horizontal (Eq. (9))	Moment of inertia point masses J (g cm^2)	Moment of inertia % of J when gaster horizontal (point mass)
(a) *Cataglyphis bicolor*				
0	3.71×10^{-3}	100	3.42×10^{-3}	100
$\pi/8$	3.53×10^{-3}	95	3.25×10^{-3}	95
$\pi/4$	3.06×10^{-3}	82	2.80×10^{-3}	82
$3\pi/8$	2.43×10^{-3}	65	2.20×10^{-3}	64
$\pi/2$	1.82×10^{-3}	49	1.60×10^{-3}	47
$5\pi/8$	1.34×10^{-3}	36	1.11×10^{-3}	32
(b) *Cataglyphis fortis*				
0	0.454×10^{-3}	100	0.350×10^{-3}	100
$\pi/8$	0.434×10^{-3}	95	0.332×10^{-3}	95
$\pi/4$	0.377×10^{-3}	83	0.285×10^{-3}	81
$3\pi/8$	0.303×10^{-3}	67	0.221×10^{-3}	63
$\pi/2$	0.229×10^{-3}	50	0.159×10^{-3}	45
$5\pi/8$	0.171×10^{-3}	38	0.110×10^{-3}	31

Table 4
Position of center of gravity and moment of inertia of (a) *Cataglyphis bicolor* and (b) *Cataglyphis fortis* with the thorax at an angle of inclination of 20° and the gaster at various angles.

Gaster angle ψ	Distance from the mandibles to the ant center of gravity L_C (mm)	Moment of inertia J (g cm^2)	Moment of inertia in % of J when gaster is horizontal
(a) *Cataglyphis bicolor*			
0	5.846	3.49×10^{-3}	100
$\pi/8$	5.748	3.32×10^{-3}	95
$\pi/4$	5.469	2.86×10^{-3}	82
$3\pi/8$	5.051	2.25×10^{-3}	64
$\pi/2$	4.559	1.66×10^{-3}	48
$5\pi/8$	4.066	1.21×10^{-3}	35
(b) *Cataglyphis fortis*			
0	3.325	0.428×10^{-3}	100
$\pi/8$	3.272	0.408×10^{-3}	95
$\pi/4$	3.120	0.353×10^{-3}	82
$3\pi/8$	2.892	0.281×10^{-3}	66
$\pi/2$	2.624	0.210×10^{-3}	49
$5\pi/8$	2.356	0.155×10^{-3}	36

The position vector, $\underline{r}_P$, in the x_1-x_2 plane for the point P is thus

$$\underline{r}_P = \underline{r} + x_P\underline{i} = x_1\underline{e}_1 + x_2\underline{e}_2 + H\underline{k} + x_P\underline{i} \qquad (12)$$

where we have used Eq. (11). Recall that $\underline{i}$ is the unit base vector parallel to the x-axis previously defined in conjunction with Eq. (4). The velocity vector, $\underline{v}_P$, in the x_1-x_2 plane of point P, with the ant's gaster at a fixed elevation, is thus

$$\underline{v}_P = \frac{d\underline{r}_P}{dt} = \frac{d\underline{r}}{dt} + x_P\frac{d\underline{i}}{dt} = \underline{v}_C + x_P\frac{d\alpha}{dt}\underline{j} = \underline{v}_C + x_P\omega\underline{j} \qquad (13)$$

where $\underline{v}_C$ is the velocity vector in the x_1-x_2 plane of the ant's center of mass, $\underline{j}$ is the unit base vector parallel to the y-axis previously defined in conjunction with Eq. (4), and α is the angle between the x_1-axis and the x-axis, i.e. between the x_1-axis and the long dimension of the ant's body as shown in Fig. 4. In Eq. (13), it has been recognized that, due to the fact that the ant must turn to follow a curved path, $d\underline{i}/dt = \underline{j}\,d\alpha/dt$, and that $d\alpha/dt$ is the angular velocity, ω, of the ant. The situation is illustrated in Fig. 4, though this figure is for a sinusoidal path that will be explored below. Nevertheless, the significance of the parameters illustrated in Fig. 4 is general.

Assume that the ant has no sideways motion, and runs at speed v parallel to its long axis, i.e. the velocity is always parallel to the x-axis (fixed in the ant) as shown in Fig. 3. However, the path may be tortuous, and the ant controls the motion of point P. Thus, we take the velocity vector, $\underline{v}_P$, of the point P within the ant to be

$$\underline{v}_P = v\underline{i} \qquad (14)$$

As a consequence, the acceleration of the center of mass of the ant is

$$\frac{d\underline{v}_C}{dt} = \left(\frac{dv}{dt} + x_P\omega^2\right)\underline{i} + (v\omega - x_P\dot\omega)\underline{j} \qquad (15)$$

where we have used $d\underline{j}/dt = -\omega\underline{i}$.

From Newtonian mechanics we then deduce that the vector force, $\underline{F}$, that the ant must apply to its body by its legs is

$$\underline{F} = m_A\left(\frac{dv}{dt} + x_P\omega^2\right)\underline{i} + m_A(v\omega - x_P\dot\omega)\underline{j} + m_A g\underline{k} \qquad (16)$$

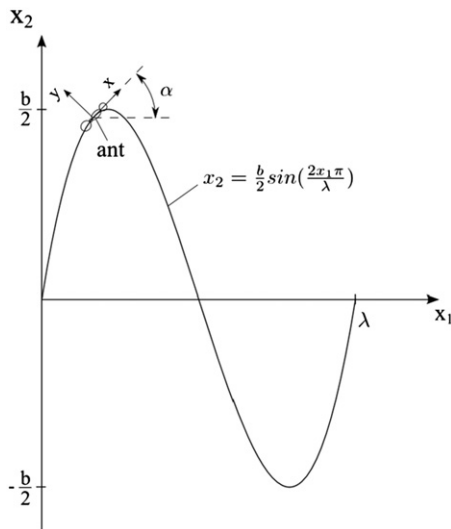where g is the gravitational acceleration and thus $m_A g$ is the ant's weight.

Fig. 4. A sinusoidal path in the x_1-x_2 plane on which the ant is assumed to run at a constant speed v.

While running on its chosen path, the ant must apply, by the thrust of its legs, a moment sufficient to ensure that it turns consistently with its trajectory. With a point in the ant's body having velocity vector $\underline{v}$, the required moment vector, $\underline{M}$, is given by the rate of change of its moment of momentum (Goldstein, 1950) and is

$$\underline{M} = \frac{d}{dt}\int_V \rho(\underline{r} + x\underline{i} + y\underline{j} + z\underline{k}) \times \underline{v}\,dV = \int_V \rho(\underline{r} + x\underline{i} + y\underline{j} + z\underline{k}) \times \frac{d\underline{v}}{dt}dV \quad (17)$$

where, for convenience, we have chosen to compute moments relative to the origin of the fixed x_1-x_2 coordinate system. Note that the term in parenthesis in Eq. (17) is the position vector of any point in the ant's body relative to the origin of the x_1-x_2 coordinate system. We may choose to use the origin of this coordinate system to enforce the condition on moments because they must be balanced relative to any point in the ant's inertial frame. We are at liberty to place the origin of the x_1-x_2 at any place we please, and so we define it instantaneously to lie vertically below the ant's center of mass Thus, instantaneously, $\underline{r} = H\underline{k}$. In view of the fact that the ant is controlling the motion of point P, and its rotation around that point, we give the velocity of each point in the ant as

$$\underline{v} = (v - \omega y)\underline{i} + \omega(x - x_P)\underline{j} \qquad (18)$$

The expression for the moment in Eq. (17) then becomes

$$\begin{aligned}
\underline{M} &= \int_V \rho\left[x\underline{i} + y\underline{j} + (H+z)\underline{k}\right] \\
&\quad \times\left\{\left[\frac{dv}{dt} - \dot\omega y - \omega^2(x-x_P)\right]\underline{i} + \left[\dot\omega(x-x_P) + \omega v - \omega^2 y\right]\underline{j}\right\}dV \\
&= \int_V \rho\left\{x\left[\dot\omega(x-x_P) + \omega v - \omega^2 y\right] - y\left[\frac{dv}{dt} - \dot\omega y - \omega^2(x-x_P)\right]\right\}\underline{k}\,dV \\
&\quad + \int_V \rho(H+z)\left\{\left[\frac{dv}{dt} - \dot\omega y - \omega^2(x-x_P)\right]\underline{j} - \left[\dot\omega(x-x_P) + \omega v - \omega^2 y\right]\underline{i}\right\}dV
\end{aligned} \qquad (19)$$

As was noted in connection with Eq. (6), the terms linear in x in Eq. (19) integrate to give zero due to the definition of the center of mass. Any term containing y, other than those in the form of y^2, integrate to give zero due to symmetry. Similarly, by the definition of the center of mass, those terms linear in z are such that

$$\int_V \rho z\,dV = m_A H_C \qquad (20)$$

As a consequence, Eq. (19) simplifies to

$$\begin{aligned}
\underline{M} &= \dot\omega\int_V \rho(x^2+y^2)dV\underline{k} + (H+H_C)\int_V \rho dV\left[\left(\frac{dv}{dt} + \omega^2 x_P\right)\underline{j} + (\dot\omega x_P - \omega v)\underline{i}\right] \\
&\quad - \int_V \rho xz\,dV(\omega^2\underline{j} + \dot\omega\underline{i}) \\
&= J\dot\omega\underline{k} + m_A(H+H_C)\left[\left(\frac{dv}{dt} + \omega^2 x_P\right)\underline{j} + (\dot\omega x_P - \omega v)\underline{i}\right] - J_t(\omega^2\underline{j} + \dot\omega\underline{i})
\end{aligned} \qquad (21)$$

where

$$J_t = \int_V \rho xz\,dV = \frac{m_H}{40}(L_H^2 - H_H^2) + \frac{1}{2}m_G r_G L_G \sin\psi + \frac{m_G}{20}(L_G^2 - H_G^2)\sin\psi\cos\psi \qquad (22)$$

is the transverse moment of inertia for the ant. The final result in Eq. (22) is given for the thorax horizontal. The value for the case where the thorax is inclined at a low angle will not differ greatly from the result given in Eq. (22). The transverse moment of inertia arises due to asymmetry of the ant, and determines, for example, the torque required around the x-axis when the ant is experiencing angular acceleration around the z-axis. It can be seen that when the gaster and the thorax are horizontal, so that $\psi = 0$, J_t is

small, reflecting the fact that then the ant's asymmetry arises solely from the head.

We thus see from Eq. (21) that the ant has to apply a torque, $J\dot\omega$, determined by its moment of inertia around its center of mass even when it controls the motion of a point P in its body other than its center of mass and determines the rotation rate around the point P. Simultaneously, the ant must arrange the thrust of its legs to apply to its body torques around the x-axis (*i.e.* the term in Eq. (21) containing $\underline{i}$) to avoid toppling sideways during turning (*i.e.* an anti-roll torque), the torque around the y-axis (*i.e.* the term in Eq. (21) containing $\underline{j}$) required to avoid toppling head over heels during acceleration and braking (*i.e.* an anti-pitch torque), and the torque around the z-axis (*i.e.* the term in Eq. (21) containing $\underline{k}$) required for the angular acceleration, *i.e.* to accelerate the rate of yawing. The yawing term is that identified previously in Eq. (5).

1.5. Estimate of forces and torques for an ant running on a circular path

Let the ant be running anti-clockwise on a circular path when viewed from above, with the circle having radius R. As a consequence, $\omega = v/R$, so that

$$\dot\omega = \frac{1}{R}\frac{dv}{dt} \tag{23}$$

Since x_P does not appear in the turning torque in Eq. (21), and because we are unsure of an appropriate location for P, we will take the value of x_p to be zero. This means that we assume that the ant can sense where its center of mass is, and adjust its motion control actions to specify how its center of mass moves. As a consequence, we can write Eq. (16) as

$$\underline{F} = m_A\frac{dv}{dt}\underline{i} + m_A\frac{v^2}{R}\underline{j} + m_A g\underline{k} \tag{24}$$

and Eq. (21) as

$$\underline{M} = -\left[m_A(H+H_C) + \frac{J_t}{R}\right]\frac{v^2}{R}\underline{i} + \left[m_A(H+H_C) - \frac{J_t}{R}\right]\frac{dv}{dt}\underline{j} + \frac{J}{R}\frac{dv}{dt}\underline{k} \tag{25}$$

It can be seen that the significance of the transverse moment of inertia, J_t, and its increase when the gaster is raised depends on the radius of the circle upon which the ant is running. If we assume that the ant runs on a circle whose diameter approximately equals the ant's length, the term J_t/R is negligible compared to $m_A H$. The increase in the transverse moment of inertia when the gaster is raised is then of no significance. It seems unlikely that the ant will run on tighter circles. Therefore, we neglect J_t/R throughout our assessment of the ant's situation.

From Eq. (25) we deduce that the ant's gaster raising is advantageous for acceleration on the circular path (J is reduced), but carries a penalty both during acceleration and constant speed running because H_C is increased. However, J can be reduced to half by the ant raising the gaster, whereas H_C increases by only about 1.3 mm for *C. bicolor* and by 0.7 mm in the case of *C. fortis* when the gaster goes from horizontal to vertical. Let us assume that H, the height of the ant's center of mass above the ground, introduced in conjunction with Eq. (11), is approximately twice the length of the gaster (see Fig. 1). In that case, $H+H_C$ increases by about 15% for both animals when the gaster is raised from horizontal to vertical. Thus the advantage of raising the gaster to cut J in half outweighs the disadvantage of the increase in $H+H_C$ that forces the ant to use a greater effort to avoid toppling.

Running for a long time in a circle at constant speed will be hampered by the increase of $H+H_C$ for the duration of the activity, whereas the advantage of a low J persists only for the spell of acceleration and braking at the beginning and end of the exercise.

It would be interesting to know if the ant raises its gaster to accelerate and brake, but lowers it at steady velocity on the circular path. In addition, we note that the circular path is different from a tortuous one in that covering the circular path at steady speed involves no angular acceleration, in contrast to the twisting back and forth that is required when the ant zig-zags. Furthermore, it seems unlikely that the ant will persist in running for long times on circular paths, as this behavior gains it little, other than perhaps a transient ability to escape a predator. For this reason, we now turn to an ant running at constant speed on a sinusoidal path possessing characteristics that typify a tortuous trajectory.

1.6. Estimate of forces and torques for an ant running at constant speed on a sinusoidal path

Let the ant's sinusoidal path have the form

$$x_2 = \frac{b}{2}\sin\frac{2x_1\pi}{\lambda} \tag{26}$$

as illustrated in Fig. 4, with b the amplitude of the sinusoid and λ its wavelength. Note that

$$\tan\alpha = \frac{dx_2}{dx_1} = \frac{\pi b}{\lambda}\cos\frac{2x_1\pi}{\lambda} \tag{27}$$

Differentiation of Eq. (27) with respect to time provides

$$\omega = -\frac{2\pi^2 bv\sin(2x_1\pi/\lambda)}{\lambda^2[1+(\pi^2 b^2/\lambda^2)\cos^2(2x_1\pi/\lambda)]^{3/2}} \tag{28}$$

where we have used $dx_1/dt = v\cos\alpha$, a result that arises by projection of the ant's velocity on the x_1-axis. We then use Eq. (15) to calculate the acceleration of the ant's center of gravity at constant speed, v, and with $x_P=0$ as

$$\frac{dv_C}{dt} = -\frac{2\pi^2 bv^2\sin(2x_1\pi/\lambda)}{\lambda^2[1+(\pi^2 b^2/\lambda^2)\cos^2(2x_1\pi/\lambda)]^{3/2}}\underline{j} \tag{29}$$

which is maximized at $x_1 = (2n-1)\lambda/4$, where n is a positive integer. Therefore the maximum magnitude of the acceleration of the ant's center of gravity is

$$\left|\frac{dv_C}{dt}\right|_{max} = \frac{2\pi^2 bv^2}{\lambda^2} \tag{30}$$

where we recall that v is the constant speed at which the ant runs along its path. The maximum in the acceleration in Eq. (30) occurs at the extremes of the amplitude of the sinusoid, where the curvature is highest, and is directed inwards from those extreme points. To support the acceleration given by Eq. (30), the ant must provide a sideways thrust by its legs, and the maximum magnitude of this force, from Newton's 2nd law, is

$$F_{max} = m_A\left|\frac{dv_C}{dt}\right|_{max} = \frac{2\pi^2 m_A bv^2}{\lambda^2} \tag{31}$$

The ant's rotational acceleration can be computed, in turn, as

$$\dot\omega = -\frac{4\pi^3 bv^2}{\lambda^3}\frac{[1+(3\pi^2 b^2/\lambda^2)-(2\pi^2 b^2/\lambda^2)\cos^2(2x_1\pi/\lambda)]\cos(2x_1\pi/\lambda)}{[1+(\pi^2 b^2/\lambda^2)\cos^2(2x_1\pi/\lambda)]^3} \tag{32}$$

Instead of considering the general situation, take $b=\lambda$, and then investigation of Eq. (32) reveals that the maximum magnitude of $\dot\omega$ occurs very close to, but not at, the amplitude extremes of the sinusoidal path, with the cosine term equal approximately to ± 0.14. The quotient of the trigonometric terms is then approximately ± 2.5, so that in this case

$$|\dot\omega|_{max} \approx 10\frac{\pi^3 v^2}{b^2} \quad \text{for} \quad \lambda = b \tag{33}$$

The ant must use its legs to apply a torque, M_z, around its z-axis (i.e. the vertical axis), from Eq. (5), with a maximum magnitude given by

$$M_z^{max} = J|\dot{\omega}|_{max} = 10J\frac{\pi^3 v^2}{b^2} \quad (34)$$

Let us assume that for *C. bicolor* the distance between its feet on one side of its body to the feet on its other side is approximately 11 mm (Zollikofer, 1988), or approximately the length, L_A, of the ant with its gaster horizontal. If we further assume that the torque in Eq. (34) is applied by the ant in the form of a couple through 2 legs, the force, P_{max}, associated with the maximum torque in Eq. (34) is given by

$$P_{max} = 10J\frac{\pi^3 v^2}{b^2 L_A} \quad (35)$$

so that the torque in Eq. (34) is produced by the couple $L_A P_{max}$. Note that *Cataglyphis* runs by a tripod (actually a bipedal) gait with 3 feet on the ground at any given time, with utilization of alternating tripods (for ants see Zollikofer, 1988, 1994; Seidl and Wehner, 2008; Weihmann and Blickhan, 2009; Reinhardt et al., 2009; for insects in general see Full and Tu, 1990, 1991; Ting et al., 1994). Therefore, we could cut the estimate in Eq. (35) down somewhat to account for the ant's use of 3 legs rather than 2, but we seek only a rough value. To compare forces expected of the ant's legs, we divide P_{max} in Eq. (35) by $F_{max}/2$ from Eq. (31), (with $\lambda = b$), with the division by 2 justified by the recognition that more than one leg will be responsible for the necessary thrust, but it may not come equally from the 3 legs of the tripod supporting the ant at any one time. We find

$$\frac{P_{max}}{F_{max}/2} = \frac{10\pi J}{m_A b L_A} = \frac{10\pi r_A^2}{b L_A} \quad (36)$$

where r_A is the radius of gyration of the ant, so that $J = m_A r_A^2$.

In the case where *C. bicolor* has its gaster held horizontal, $L_A \approx 11$ mm, $r_A \approx 3.56$ mm so that $r_A/L_A \approx 1/3$. The ratio is similar for *C. fortis*. As a result, the ratio of forces in Eq. (36) is

$$\left(\frac{P_{max}}{F_{max}/2}\right)_{gaster\ horizontal} \approx \frac{\pi L_A}{b} \quad (37)$$

It is difficult to judge what the ant can tolerate, but for the sake of argument let us assume that it can afford to have this parameter equal to unity, i.e. the ant can apply the same level of force parallel to the ground sideways and fore and aft when it maneuvers through a turn. With the left hand side of Eq. (37) thus set to unity, we then deduce that the ant can afford to run on a sinusoidal path for which the amplitude and wavelength are about 3 times greater than its body length, i.e. we obtain $b \approx 3L_A$ from Eq. (37), having approximated π as 3.

Now consider the ant when it has its gaster vertical. In this case $r_A/L_A \approx 1/4$ and

$$\left(\frac{P_{max}}{F_{max}/2}\right)_{gaster\ vertical} \approx \frac{\pi L_A}{2b} \quad (38)$$

If we use the same criterion as above, the ant can now tolerate sinusoidal paths that are twice as severe, with amplitude and wavelength that are only about 1.5 times its full (gaster horizontal) body length, and consequently having tighter turns than those the ant can follow with its gaster horizontal.

Now consider the question of toppling. The moment that the ant must apply to its body by its legs when it is running on a tortuous path at constant speed is, from Eq. (21)

$$\underline{M} = J\dot{\omega}\underline{k} - m_A(H+H_C)\omega v\underline{i} \quad (39)$$

where we have omitted the terms containing the transverse moment of inertia, J_t, as the curvature of the paths will not be

sufficient to make this term important. The term containing $\underline{i}$ is that required to ensure that the ant does not topple sideways, and is thus the x-component

$$M_x = -m_A(H+H_C)\omega v \quad (40)$$

of the moment vector, i.e. the moment applied by the ant around its (lengthwise) x-axis. From the deductions in the sequence Eqs. (28)–(30), the maximum value of this component is

$$(M_x)_{max} = \frac{2\pi^2 m_A(H+H_C)v^2}{\lambda} \quad (41)$$

where we have used the assumption $\lambda = b$ introduced above. This moment is applied by the ant by supporting more of its weight on the legs on one side of its body. If we assume all of the ant's weight is supported by the legs on one side of the body and none on the other, we have the maximum moment that the ant can exert. The lever arm for this moment from the ant's center of mass to the positions of its footfalls is approximately half of the ant's length (Zollikofer, 1988). Therefore, we use $(M_x)_{max} = m_A g L_A/2$ and obtain the maximum feasible velocity from Eq. (41) as

$$v_{max} = \frac{1}{2\pi}\sqrt{\frac{gL_A\lambda}{(H+H_C)}} \quad (42)$$

With the gaster horizontal, we deduced above that the ant can follow a path on which $\lambda \approx 3L_A$, and since $H_C = 0$ in this case, we obtain a maximum speed of

$$v_{max} = \frac{1}{\pi}\sqrt{gL_A} \quad (43)$$

where we have used the rough estimate $H = 3L_A/4$, consistent with our previous assumption that $H \approx 2L_G$. For *C. bicolor*, the result in Eq. (43) is approximately 0.1 m/s. This speed requires a sideways thrust of 0.17 mN at the extremes of the sinusoidal path, as computed from Eq. (31), given the parametric values deduced above.

Now consider the ant with the gaster vertical. In this case, we estimated that the ant can follow a path with $\lambda \approx 3L_A/2$, and this reduces the ant's maximum feasible speed to 70% of the estimate in Eqs. (42) and (43), or 0.07 m/s for *C. bicolor*. The complete result for the case of the gaster raised is

$$v_{max} = \frac{1}{\pi}\sqrt{\frac{gL_A}{2.3}} = \frac{0.66}{\pi}\sqrt{gL_A} \quad (44)$$

where we have used $H+H_C = 1.15H$ for the case where the gaster is raised, consistent with our observation above in the context of the ant running in a circle. The result in Eq. (44) gives a value of 0.66 m/s for the maximum velocity of *C. bicolor* with the gaster raised, or a mere penalty of just over 5% on the top feasible speed. This assessment confirms that ant gains much in terms of maneuverability by raising the gaster since it eases its ability to increase its angular acceleration. At the same time the ant pays only a modest penalty in terms of its resistance to toppling sideways, due to the fact that raising the gaster heightens the ant's center of mass by a small fraction of the height of its legs.

2. Discussion

The large workers of *Cataglyphis bicolor* and the significantly smaller workers of *Cataglyphis fortis* are two prime examples of desert ants that are able to raise the hind part of their bodies, the gaster (metasoma), to a fully upright position (Fig. 1). In the latter species the gaster can be tilted upward by even more than 90°, so that its posterior tip points forward (Fig. 1 on left). This remarkable behavior is largely facilitated by a derived morphological trait, the cubiform shape of the petiole. Dlusskij (1981) has shown what

modifications the petiolar muscle system had to undergo in order to enable the animal to elevate its gaster. On the behavioral side, the ability of raising the gaster is associated with high running speeds including both translatory and rotatory movements.

Using geometric models based on morphological data (dimensions and masses of the individual body parts) of both species of desert ant, we have tested the hypothesis put forward by Wehner (1983) that the upright position of the gaster brings the heavy mass of this hind part of the body closer to the animal's turning axis and thus decreases the moment of inertia. Our mechanical analysis shows indeed that, by raising its gaster, both species of ants can reduce their moment of inertia to about one half. Moreover, analysis of forces on an ant running on a sinusoidal path has demonstrated that the ant can take tighter turns when its gaster is raised. The ants are often observed to run in straight paths with the gaster raised slightly up to about $\psi = \pi/4$. When this is used as the datum, the advantage of raising the gaster to the vertical position is less than the 50% reduction of the moment of inertia that we have ascertained as the difference between the horizontal and vertical positions. If the gaster goes from $\psi = \pi/4$ to the vertical position, the reduction of the moment of inertia is approximately 40%, i.e. the ant's moment of inertia with the gaster vertical is approximately 60% of its value when the gaster is at $45°$. Thus, there is still a substantial reduction. Furthermore, if the gaster goes from $\psi = \pi/4$ to $\psi = 5\pi/8$ so that it is inclined towards the thorax, as is observed, the reduction of the moment of inertia is around 60%, i.e. the ant's moment of inertia with the gaster at $\psi = 5\pi/8$ is approximately 40% of its value when the gaster is at $45°$. Therefore, the ant has strategies available to it to reduce its moment of inertia by a factor of 2 whether it starts with the gaster horizontal or at $45°$.

As to a different kind of argument, it has been claimed that raising the gaster is "to protect the vital organs contained in it from high temperatures" (Cerdá, 2001). This is an unlikely hypothesis for a number of reasons. First, the vital organs most susceptible to heat stress are the gonads and the brain, but in ant workers (which are all females) the ovaries are not developed, and the brain is housed at the opposite end of the body. Second, if Cataglyphis ants are exposed to gradually rising temperatures (by the dynamic method: Lutterschmidt and Hutchison, 1997), the ant's body temperature increases, but from a certain critical temperature it is the head rather than the gaster that, by evaporative cooling, is kept at a lower temperature than the rest of the body. Once this critical temperature is reached, the ants regurgitate a droplet of fluid from the mouth or the anus and spread it with their legs across the surface of the head (thermovision recordings by S. Heinzelmann and R. Wehner, unpublished data). Thirdly, the most heat-tolerant of all Cataglyphis species – the sand-dune species Cataglyphis bombycina and Cataglyphis pallida – have a squamiform petiole and do not raise the gaster, while the northern Mediterranean Cataglyphis noda, which inhabits more mesic (macchie, bushland and even agricultural) areas, where it rapidly walks over rugose ground, is provided with a nodiform petiole and is able to raise its gaster. Even though all these arguments provide only circumstantial evidence, taken together they make it very unlikely indeed that the evolutionary driving force for the gaster-raising habit has been heat avoidance. Rather, as shown in the present account, the whole suite of adaptations of the locomotor apparatus that finally result in the ant's ability to elevate the gaster whenever the animal is in its fast and tortuous running mode, favor the hypothesis scrutinized in the present account: what the ants gain in raising their gaster is an increase in energetically efficient locomotor agility.

In conclusion, whatever the criterion for how big the torque/ thrust force ratio, i.e., the ratio of the turning force to the sideways thrust force can be, with its gaster vertical, the ant can tackle tighter turns than with its gaster horizontal, to the extent of increasing its angular acceleration by a factor of 2. As a result, regular, programmed paths such as a sinusoid, which the ant may follow when scavenging for food, can be tighter, and the ant can move along them faster. Similarly, erratic paths involving abrupt, unpredictable turns, such as those the ant may adopt when it is fleeing from a predator, can be more tortuous and have more acute diversions. In both circumstances, it is logical to infer that the ability to raise its gaster to a vertical position, and to pursue tighter turns as a result, bestows on the ant an evolutionary advantage. The latter conclusion is nicely corroborated by the fact that the trait of raising the gaster is restricted to the worker caste. It does not occur in the sexual forms, the males and (fertile) females. While the workers of both Cataglyphis species considered here get engaged in far-ranging foraging journeys (Wehner, 1987), have relatively long legs (Sommer and Wehner, 2011) and a cubiform petiole, the sexual individuals of the two species disperse by flying, have relatively short legs and a squamiform petiole that prevents them from elevating the gaster (Wehner, 1983).

References

Agosti, D., 1990. Review and reclassification of Cataglyphis (Hymenoptera, Formicidae). J. Nat. Hist. 24, 1457–1505.

Cerdá, X., 2001. Behavioral and physiological traits to thermal stress tolerance in two Spanish desert ants. Etologia 9, 15–27.

Duelli, P., 1975. A fovea for e-vector orientation in the eye of Cataglyphis bicolor (Formicidae, Hymenoptera). J. Comp. Physiol. 102, 43–56.

Dlusskij, G.M., 1981. The Ants of the Desert. Academia Nauk USSR, Moscow (in Russian).

Full, R.J., Tu, M.S., 1990. Mechanics of six-legged runners. J. Exp. Biol. 148, 129–146.

Full, R.J., Tu, M.S., 1991. Mechanics of rapid running insects: two-, four- and six-legged locomotion. J. Exp. Biol. 156, 215–231.

Goldstein, H., 1950. Classical Mechanics. Addison-Wesley, Reading, Massachusetts.

Lutterschmidt, W.J., Hutchison, V.H., 1997. The critical thermal maximum: history and critique. Can. J. Zool. 75, 1561–1574.

Reinhardt, L., Weihmann, T., Blickhan, R., 2009. Dynamics and kinematics of ant locomotion: do wood ants climb on level surfaces? J. Exp. Biol. 212, 2426–2435.

Seidl, T., Wehner, R., 2008. Walking on inclines: how do desert ants monitor slope and step length. Front. Zool. 5, 8. doi:10.1186/1742-9994-5-8.

Sommer, S., Wehner, R., 2011. Leg allometry in ants: extreme long-legedness in thermophilic species. Arthropod Struct. Dev.. doi:10.1016/j.asd.2011.08.002.

Ting, L.H., Blickhan, R., Full, R.J., 1994. Dynamic and static stability in hexapedal runners. J. Exp. Biol. 197, 251–269.

Wehner, R., 1982. Himmelsnavigation bei Insekten. Neurophysiologie und Verhalten. Neujahrsblatt Naturforsch. Ges. Zürich 184, 1–132.

Wehner, R., 1983. Taxonomie,Funktionsmorphologie und Zoogeographie der saharischen Wüstenameise Cataglyphis fortis (Forel 1902) stat. nov. (Insecta: Hymenoptera: Formicidae). Senckenbergiana Biol. 64, 89–132.

Wehner, R., 1987. Spatial organization of foraging behavior in individually searching desert ants, Cataglyphis (Sahara Desert) and Ocymyrmex (Namib Desert). In: Pasteels, J.M., Deneubourg, J.-L. (Eds.), From Individual to Collective Behavior in Social Insects. Birkhäuser, Basel, Boston, pp. 15–42.

Wehner, R., Fukushi, T., Isler, K., 2007. On being small: ant brain allometry. Brain Behav. Evol. 69, 220–228.

Wehner, R., Wehner, S., 1990. Insect navigation: use of maps or Adriane's thread? Ethol Ecol. Evol. 2, 27–48.

Wehner, R., Wehner, S., Agosti, D., 1994. Patterns of biogeographic distribution within the bicolor species group of the North African desert ant, Cataglyphis FOERSTER 1850 (Insecta: Hymenoptera: Formicidae). Senckenbergiana Biol. 74, 163–191.

Weihmann, T., Blickhan, R., 2009. Comparing inclined locomotion in a ground-living and a climbing ant species: sagittal plane kinematics. J. Comp. Physiol. A 195, 1011–1020.

Zollikofer, C.P.E., 1988. Vergleichende Untersuchungen zum Laufverhalten von Ameisen (Hymenoptera: Formicidae). Ph.D. Thesis. University of Zürich.

Zollikofer, C.P.E., 1994. Stepping patterns in ants. I. Influence of speed and curvature. J. Exp. Biol. 192, 95–106.